

## Observation of Collective-Emission-Induced Cooling of Atoms in an Optical Cavity

Hilton W. Chan, Adam T. Black, and Vladan Vuletić

*Department of Physics, Stanford University, Stanford, California 94305-4060*

(Received 10 April 2002; revised manuscript received 15 August 2002; published 14 February 2003)

We report the observation of collective-emission-induced, velocity-dependent light forces. One-third of a falling sample containing  $3 \times 10^6$  cesium atoms illuminated by a horizontal standing wave is stopped by cooperatively emitting light into a vertically oriented, confocal resonator. We observe decelerations up to  $1500 \text{ m/s}^2$  and cooling to temperatures as low as  $7 \mu\text{K}$ , well below the free-space Doppler limit. The measured forces substantially exceed those predicted for a single two-level atom.

DOI: 10.1103/PhysRevLett.90.063003

PACS numbers: 32.80.Pj, 32.80.Lg

In conventional free-space Doppler cooling [1], a two-level atom irradiated with laser light tuned slightly below the atomic-transition frequency preferentially absorbs photons from the beam opposing the atom's velocity. The associated momentum transfer from the incident light onto the atom results in a velocity-dependent, absorptive force for the atom's center-of-mass motion.

For atoms inside a resonator, the frequency variation of the electromagnetic mode density, and consequently of the atomic emission rate [2–5], can give rise to emission-induced forces [6–13], as observed for a single atom in a high-finesse resonator [10]. In the classical limit of low atomic-transition saturation, cavity Doppler cooling may occur [8,11]: A dissipative force arises from the two-photon momentum transfer in coherent scattering, i.e., from the combined absorption and reemission process. The atom will be cooled if the cavity is blue detuned relative to the incident light by the two-photon Doppler shift, thereby enhancing the emission of high-energy photons [12]. The light-atom detuning and the atomic structure determine only the scattering rate and hence the cooling force magnitude [11].

More generally, cooling will occur whenever the average emitted light frequency exceeds the incident frequency. An interesting situation arises in the presence of intracavity gain provided by a many-atom system, which can lead to collective emission into the resonator. The optical gain amplifies the resonator-induced force  $f$ , while the reduced bandwidth [14] increases the velocity dependence  $\partial f/\partial v$  via stronger discrimination between the red and blue Doppler sidebands. Both of these features should improve the cooling performance.

In this Letter, we report on the first observation of collective-emission-induced, velocity-dependent forces acting on atoms inside a resonator. The resonator-induced slowing and cooling of  $10^6$  cesium atoms is accompanied by cooperative emission into a near-confocal resonator. A deceleration of  $1500 \text{ m/s}^2$  is measured along the resonator axis, perpendicular to the incident light. Neither the collective emission nor the observed temperatures down to  $7 \mu\text{K}$  can be explained by a single-atom model of cavity Doppler cooling [8,11] that, for our parameters,

predicts decelerations below  $100 \text{ m/s}^2$  and temperatures near  $200 \mu\text{K}$  [12]. Our observations suggest that the cavity-induced force is substantially enhanced by stimulated emission.

At the heart of the experiment [Fig. 1(a)] is a vertically oriented, nearly confocal optical resonator with a finesse  $F = 1000$ , length  $L = 7.5 \text{ cm}$ , and  $\text{TEM}_{00}$  waist size  $w_0 = 101 \mu\text{m}$ . One cavity mirror is mounted on a piezoelectric tube providing more than one free spectral range ( $c/2L = 2 \text{ GHz}$ ) of cavity tuning. From the cavity's spatial transmission pattern [15], we estimate our cavity to be  $24 \mu\text{m}$  ( $28 \mu\text{m}$ ) short of confocality in the  $x$  ( $y$ ) direction, where the difference is due to stress-induced asymmetric mirror curvature. Mirror spherical aberration leads to a quadratic dependence of the mode frequency on transverse mode number [16], broadening the cavity spectrum to about  $200 \text{ MHz}$ . The nonconfocal geometry and spherical aberration produce a maximum in mode density at a detuning of  $-200 \text{ MHz}$  relative to the  $\text{TEM}_{00}$  mode, where the resonant volume [5,15] is  $2.5 \text{ mm} \times 800 \mu\text{m} \times 7.5 \text{ cm}$  in the  $x$ ,  $y$ , and  $z$  directions, respectively.

The incident beams are derived from a tunable diode laser operating near  $852 \text{ nm}$ , whose linewidth is narrowed via optical feedback [17] to less than  $10 \text{ kHz}$ . Its frequency is actively stabilized relative to a Cs atomic transition. A linearly polarized standing wave, formed by a

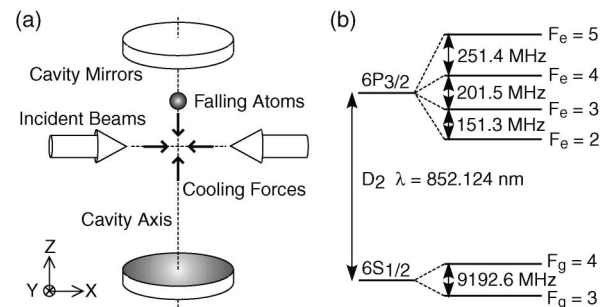


FIG. 1. (a) Experimental setup for observing emission-induced forces. Cs atoms, illuminated by two horizontal laser beams and falling along the resonator, experience velocity-dependent forces in the  $xz$  plane. (b) Cs hyperfine structure.

retroreflected, horizontal beam with 600  $\mu\text{m}$  waist and single-beam power of up to 16 mW, intersects the cavity axis near the cavity center. A small fraction of the light is coupled into the resonator to electronically lock the laser-cavity detuning  $\Delta_c = \omega_i - \omega_c$ , where  $\omega_i$  and  $\omega_c$  are the angular frequencies of the incident light and the nearest  $\text{TEM}_{00}$  cavity resonance, respectively. During each measurement, the locking light is turned off.

We begin each measurement by collecting  $3 \times 10^6$  Cs atoms in a magneto-optical trap (MOT) and dropping them from a variable height (0 to 5 mm) above the cavity center. The available drop time is limited by the thermal cloud expansion that reduces the overlap with the resonant cavity modes. Upon reaching the cavity center with a velocity  $v_0$  between 0 and 30 cm/s and a cloud size between 400  $\mu\text{m}$  and 1.2 mm, the atoms are illuminated for durations between 100  $\mu\text{s}$  and 25 ms. The incident light is red detuned up to  $\delta_a/2\pi = -160$  MHz relative to the atomic  $F_g = 4 \rightarrow F_e = 5$  transition [Fig. 1(b)], which has a natural linewidth  $\Gamma/2\pi = 5.3$  MHz. Simultaneously, the MOT repumping laser is applied on the  $F_g = 3 \rightarrow F_e = 4$  transition to keep the atoms in the upper hyperfine state  $F_g = 4$ . Finally, we perform a time-of-flight (TOF) measurement of the atomic velocity distribution using a light sheet 2 cm below the incident beams [18] or fluorescence imaging in the  $xz$  plane.

The signature of a resonator-induced force on the atoms is a second, delayed peak in the TOF signal (Fig. 2, inset), appearing only for incident light frequencies within the cavity spectrum  $-200 \text{ MHz} < \Delta_c/2\pi < 0$ . The delayed TOF peak corresponds to a slowed or stopped cloud containing up to 30% (15%) of the original MOT atom number for vertical (horizontal) polarization of the incident standing wave. Tuning the cavity off resonance, we find only heating at a rate consistent with recoil heating by free-space scattering. A spatial image, taken 10 ms after the exposure, reveals two separate falling clouds. Figure 2 shows  $t_f$ , the time between the extinction of the incident light and the arrival of the delayed peak at the TOF beam, as a function of light

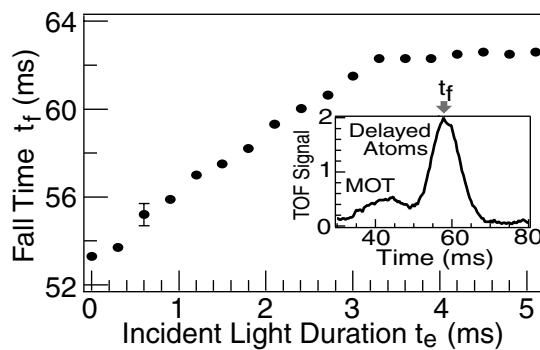


FIG. 2. Fall time  $t_f$  of atoms with  $v_0 = 15$  cm/s versus light exposure time  $t_e$  for  $\Delta_c/2\pi = -150$  MHz,  $I/I_s = 16$ , and  $\delta_a/2\pi = -63$  MHz. The inset shows the TOF signal of the remnant MOT cloud and the delayed atoms for  $t_e = 2$  ms.

exposure time  $t_e$  for  $\Delta_c/2\pi = -150$  MHz, an initial velocity  $v_0 = 15$  cm/s, a light-atom detuning  $\delta_a/2\pi = -63$  MHz, and a single-beam peak intensity  $I = 16I_s$ , where  $I_s = 1.1$  mW/cm<sup>2</sup> is the saturation intensity for unity oscillator strength. For short times  $t_e$ , the positive slope  $\partial t_f/\partial t_e$  indicates that the atoms decelerate from  $v_0$ , while the constant fall time  $t_f$  for  $t_e > 3.3$  ms indicates a stopped cloud. The atoms can be suspended for up to 25 ms. Slowing occurs only for incident beam detuning  $-160 \text{ MHz} < \delta_a/2\pi < -15$  MHz and an exact retro-reflection. For a misalignment of a few mrad, the atoms are accelerated downward or even upward (arriving up to 10 ms before the remnant MOT cloud, or up to 5 ms later than a stopped cloud). With increasing atomic scattering rate  $\Gamma_{fs}$ , the deceleration grows. At  $\Gamma_{fs} = 3 \times 10^6 \text{ s}^{-1}$ , atoms with a velocity of 15 cm/s are stopped in 100  $\mu\text{s}$ , indicating a deceleration of 1500 m/s<sup>2</sup>.

Using two photodiodes, we measure the ratio  $\eta = \Gamma_c/\Gamma_{fs}$  of the emission rates into a single cavity direction  $\Gamma_c$  and into free-space  $\Gamma_{fs}$  (Fig. 3). Surprisingly, whenever the atoms are delayed, we observe collective emission into the cavity, as identified by a sharp increase in  $\eta$  above a threshold incident intensity  $I_{th}$ . We find that  $I_{th}$  is proportional to  $\delta_a^2$ , and that it corresponds to a saturation parameter  $p = (I/I_s)\Gamma^2/(4\delta_a^2 + \Gamma^2) \approx 0.03$  and  $\Gamma_{fs} \approx pC\Gamma/2 = 2 \times 10^5 \text{ s}^{-1}$  per atom for  $10^6$  atoms and a MOT temperature  $T_{\text{MOT}} = 10 \mu\text{K}$ . Here  $C = 11/27$  is the  $F_g = 4 \rightarrow F_e = 5$  transition oscillator strength for linearly polarized light. While slowing is observed only for  $\delta_a < 0$ , collective emission occurs for both  $\delta_a < 0$  and  $\delta_a > 0$ . Varying the drop height and  $T_{\text{MOT}}$ , we find  $I_{th}$  is independent of the mean initial velocity  $v_0$  of the falling cloud and is proportional to  $T_{\text{MOT}}$  in the region  $7 \mu\text{K} < T_{\text{MOT}} < 30 \mu\text{K}$ . As the atomic transition approaches saturation, the ratio  $\eta$  slowly decreases. For emission into the  $\text{TEM}_{00}$  mode, the intracavity peak intensity just above threshold is typically 120 mW/cm<sup>2</sup>.

The increase in cavity emission rate  $\Gamma_c = \eta\Gamma_{fs}$  implies a possible enhancement over the single-atom cooling

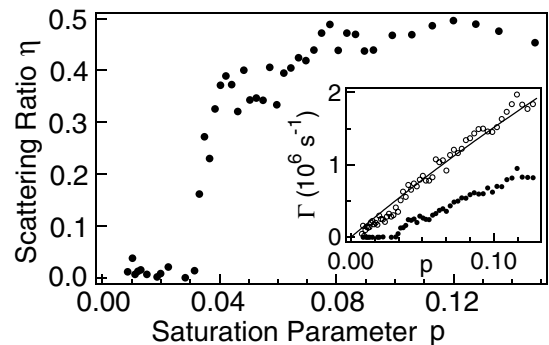


FIG. 3. Scattering ratio  $\eta = \Gamma_c/\Gamma_{fs}$  versus atomic saturation parameter  $p$  for  $10^6$  atoms,  $\delta_a/2\pi = -78$  MHz, and  $\Delta_c/2\pi = -150$  MHz. The inset shows the scattering rate into free space  $\Gamma_{fs}$  (open circles) and into the cavity  $\Gamma_c$  (solid circles) per atom. The solid line is the calculated  $\Gamma_{fs}$ .

force. In our near-confocal setup with frequency-dependent mode density  $\rho(\omega)$ , the value of  $\eta$  varies with laser-cavity detuning  $\Delta_c$ . Below the collective-emission threshold, we find a maximum  $\eta_s \approx 0.05$  near  $\Delta_c = -200$  MHz, consistent with a value derived from the measured  $\rho(\omega)$  and TEM<sub>00</sub> linewidth  $\kappa/2\pi = 1$  MHz [12]. Above threshold, we observe  $\eta_c \approx 1$ . For a single atom moving at  $v_0 = 15$  cm/s, the expected deceleration [12] is  $a_s = 2\eta_s\Gamma_{fs}v_{\text{rec}}kv_0/\kappa = 90$  m/s<sup>2</sup> at  $\Gamma_{fs} = 3 \times 10^6$  s<sup>-1</sup>, where  $v_{\text{rec}} = 3.5$  mm/s is the recoil velocity, and  $2\pi/k = 852$  nm. The 17 times larger measured value  $a = 1500$  m/s<sup>2</sup> suggests that the collective emission with  $\eta_c/\eta_s = 20$  may be responsible for the large observed force.

Raman lasing between magnetic sublevels [19] can explain the sudden increase in  $\eta$ . Linearly polarized incident light on an  $F \rightarrow F + 1$  transition optically pumps the atoms toward states of lower magnitude  $|m|$  of the magnetic quantum number  $m$  along the polarization axis [20], resulting in Raman gain [21] on the transition  $|F_g = 4, m\rangle \rightarrow |F_e = 5, m\rangle \rightarrow |F_g = 4, m'\rangle$  and loss on  $|4, -m\rangle \rightarrow |5, -m'\rangle \rightarrow |4, -m'\rangle$ , where  $m' = m + 1$  ( $m' = m - 1$ ) for  $m \geq 0$  ( $m \leq 0$ ). When the  $m$ -dependent light shifts are included, the Raman gain and absorption occur at different frequencies, yielding net gain for circularly polarized light at a frequency  $\omega_e$  satisfying the Raman resonance condition [21], where for our parameters  $|\omega_e - \omega_i| \leq \kappa, \Gamma$ .

Several observations agree with this interpretation. For incident  $z$ -polarized light, the atoms emit twice as much circularly polarized light into the vertical direction as for incident horizontal polarization [14,22], leading to stronger lasing and more slowed atoms. For  $z$  polarization, a magnetic field of 0.4 G applied in the  $xy$  plane inhibits laser action by causing Larmor precession that destroys the population inversion, while similar vertical fields enhance the laser emission. We observe that the light exiting the cavity is mostly unpolarized, with residual polarizations of 8(1)% along  $y$  and 10(3)% circular, consistent with a largely incoherent superposition of  $\sigma^+$  and  $\sigma^-$  light. Further, using microwave transitions  $|F_g = 4, m\rangle \rightarrow |F_g = 3, m\rangle$  and fluorescent detection on the  $F_g = 3 \rightarrow F_e = 2$  transition, we find that the population ratio of magnetic sublevels changes above the lasing threshold. Finally, the observed cessation of collective emission at large red detuning  $\delta_a/2\pi < -160$  MHz is explained by depolarization of the atomic sample due to excitation to the  $F_e = 4$  hyperfine excited manifold and decay to  $F_g = 3$  [Fig. 1(b)].

Varying the light exposure time, we observe both a slowing of the cloud and a changing width of the delayed Gaussian TOF peak (Fig. 2). Shown in Fig. 4 is the temperature evolution for  $\Delta_c/2\pi = -150$  MHz,  $I/I_s = 20$ , and  $\delta_a/2\pi = -78$  MHz. During the evolution, the number of delayed atoms changes by less than 50%. The time constant  $\tau = 0.4$  ms is about 100 times longer than the scattering time. We observe vertical temperatures

$T_z = 16$   $\mu$ K for instantaneous incident-light extinction, and  $T_z = 7$   $\mu$ K for slow extinction with a time constant longer than 0.4 ms. Similar final temperatures are observed for initial temperatures up to 60  $\mu$ K. By spatially imaging the falling atoms, we find that cooling also occurs along the incident light direction, as predicted by cavity Doppler cooling [12]. For example, for an initial temperature of 46  $\mu$ K (51  $\mu$ K) in the  $x$  ( $z$ ) direction and sudden incident-light extinction, we measure a final temperature of 20  $\mu$ K (14  $\mu$ K). In contrast to polarization gradient cooling [20], the final temperature is largely independent of beam intensity and light-atom detuning  $\delta_a$  for  $-160$  MHz  $< \delta_a/2\pi < -50$  MHz, and only increases as the atomic transition approaches saturation (Fig. 5).

Although the resonator-induced forces do not result in temperatures significantly below  $T_{\text{MOT}}$ , they counteract the substantial heating otherwise caused by free-space scattering. For instance, for an off-resonant cavity the final temperature after 5 ms for the parameters of Fig. 4 is 125  $\mu$ K. Therefore the observed temperature and approximately constant atom number cannot be explained by mere filtering from the MOT velocity distribution and trapping in the intracavity standing wave.

The single-atom model of cavity cooling [8] predicts a friction force only in a region of steep positive cavity slope  $\partial\eta/\partial\omega$ , where the scattering into the cavity increases rapidly with emission frequency  $\omega$  [11]. In contrast, we observe slowing and cooling for emission into transverse cavity modes with mode indices ranging from 0 to 500, as determined by  $\Delta_c$ . This mode-independent cooling suggests that our particular cavity geometry is not imperative. Further, the observed temperature is 20 times lower than the expected final value [12]  $T_{s,z} = \hbar\kappa/(10k_B\eta_s) \approx 190$   $\mu$ K. For an off-resonant cavity, only heating is observed, indicating that the incident light does not decelerate, trap or cool the atoms independently of the resonator. Conventional cooling mechanisms cannot produce strong dissipative forces in the vertical direction, perpendicular to the applied laser beams.

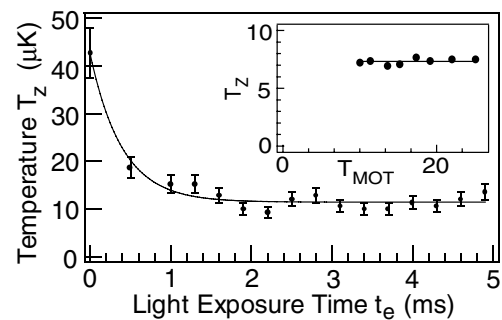


FIG. 4. Evolution of the delayed atom sample's vertical temperature  $T_z$  for  $\Delta_c/2\pi = -150$  MHz,  $I/I_s = 20$ ,  $\delta_a/2\pi = -78$  MHz. The inset shows  $T_z$  versus initial MOT temperature  $T_{\text{MOT}}$  in  $\mu$ K for  $I/I_s = 13$  and  $\delta_a/2\pi = -58$  MHz with all other parameters as given in Fig. 5.

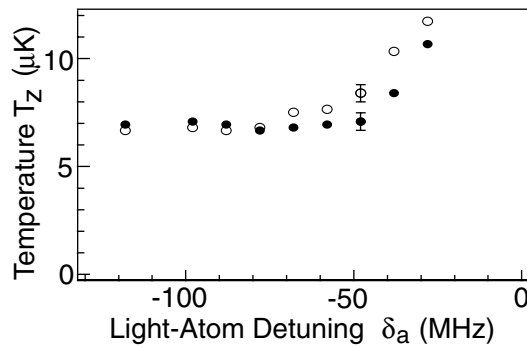


FIG. 5. Vertical temperature  $T_z$  versus  $\delta_a$  for  $I/I_s = 22$  (open) and  $I/I_s = 11$  (solid) along with typical error bars. All data were taken with  $10^6$  atoms for  $\Delta_c/2\pi = -200$  MHz, 5 ms exposure time, and slow light extinction within 0.4 ms.

Free-space Doppler cooling in our standing wave at  $\delta_a/2\pi = -160$  MHz should lead to a horizontal temperature [18] of 3.8 mK, more than 300 times higher than the observed value.

Lower  $x$  temperatures could be achieved by sub-Doppler cooling [18,20], but the incident light contains no polarization gradients and the intracavity light is almost unpolarized. Because of Doppler effects and Zeeman shifts of up to 200 kHz, as well as the incident-beam-induced differential light shift  $\Delta U/h \approx 100$  kHz between magnetic sublevels, any polarization interference pattern between the intracavity and incident light is not stationary. Using a weak probe beam transmitted through the resonator, we have also directly verified for a falling cloud that there is no optical gain at the incident frequency  $\omega_i$ . The observed forces can therefore not be explained by conventional polarization gradient cooling. However, a novel form of sub-Doppler cooling involving time-varying polarization gradients acting on nondegenerate magnetic sublevels cannot be excluded.

In conclusion, we have observed collective emission from cold atoms inside an optical resonator, accompanied by velocity-dependent forces that are significantly stronger than expected for single atoms. A model must account for both the weak dependence on cavity slope and the requirement of negative light-atom detuning. Possible explanations include self-organization of the atoms into patterns that maximize collective scattering [23], or the joint effects of cavity tuning by the moving atoms [8] and coherent Raman scattering, possibly in combination with laser mode competition between the blue and red Doppler emission sidebands.

This work was supported in part by the ARO. We thank Xinan Wu for technical assistance and Cheng Chin for stimulating discussions.

- [1] T.W. Hänsch and A. L. Schawlow, *Opt. Commun.* **13**, 68 (1975).
- [2] E. M. Purcell, *Phys. Rev.* **69**, 681 (1946).
- [3] D. Kleppner, *Phys. Rev. Lett.* **47**, 233 (1981).
- [4] P. Goy, J. M. Raimond, M. Gross, and S. Haroche, *Phys. Rev. Lett.* **50**, 1903 (1983); R. G. Hulet, E. S. Hilfer, and D. Kleppner, *ibid.* **55**, 2137 (1985); W. Jhe, A. Anderson, E. A. Hinds, D. Meschede, L. Moi, and S. Haroche, *ibid.* **58**, 666 (1987).
- [5] D. J. Heinzen, J. J. Childs, J. E. Thomas, and M. S. Feld, *Phys. Rev. Lett.* **58**, 1320 (1987); D. J. Heinzen and M. S. Feld, *ibid.* **59**, 2623 (1987).
- [6] T.W. Mossberg, M. Lewenstein, and D. J. Gauthier, *Phys. Rev. Lett.* **67**, 1723 (1991); M. Lewenstein and L. Roso, *Phys. Rev. A* **47**, 3385 (1993).
- [7] J. I. Cirac, A. S. Parkins, R. Blatt, and P. Zoller, *Opt. Commun.* **97**, 353 (1993); J. I. Cirac, M. Lewenstein, and P. Zoller, *Phys. Rev. A* **51**, 1650 (1995).
- [8] P. Horak, G. Hechenblaikner, K. M. Gheri, H. Stecher, and H. Ritsch, *Phys. Rev. Lett.* **79**, 4974 (1997).
- [9] M. Gangl, P. Horak, and H. Ritsch, *J. Mod. Opt.* **47**, 2741 (2000); G. Hechenblaikner, M. Gangl, P. Horak, and H. Ritsch, *Phys. Rev. A* **58**, 3030 (1998); M. Gangl and H. Ritsch, *ibid.* **61**, 011402 (2000); **61**, 043405 (2000); **64**, 063414 (2001); *Eur. Phys. J. D* **8**, 29 (2000); P. Domokos, P. Horak, and H. Ritsch, *J. Phys. B* **34**, 187 (2001).
- [10] P. Münstermann, T. Fischer, P. Maunz, P.W.H. Pinkse, and G. Rempe, *Phys. Rev. Lett.* **82**, 3791 (1999); C. J. Hood, T.W. Lynn, A. C. Doherty, A. S. Parkins, and H. J. Kimble, *Science* **287**, 1447 (2000).
- [11] V. Vuletić and S. Chu, *Phys. Rev. Lett.* **84**, 3787 (2000).
- [12] V. Vuletić, H.W. Chan, and A.T. Black, *Phys. Rev. A* **64**, 033405 (2001).
- [13] F. A. Narducci, Z. X. Ye, and H. Y. Ling, *J. Mod. Opt.* **49**, 687 (2002).
- [14] A. E. Siegman, *Lasers* (University Science Books, Sausalito, 1986).
- [15] M. Hercher, *Appl. Opt.* **7**, 951 (1968).
- [16] V.F. Lazutkin, *Opt. Spectrosc.* **24**, 236 (1968) [*Opt. Spektrosk.* **24**, 453 (1968)].
- [17] B. Dahmani, L. Hollberg, and R. Drullinger, *Opt. Lett.* **12**, 876 (1987).
- [18] P. D. Lett, R. N. Watts, C. I. Westbrook, W. D. Phillips, P. L. Gould, and H. J. Metcalf, *Phys. Rev. Lett.* **61**, 169 (1988).
- [19] C. K. N. Patel and E. D. Shaw, *Phys. Rev. B* **3**, 1279 (1971).
- [20] J. Dalibard and C. Cohen-Tannoudji, *J. Opt. Soc. Am. B* **6**, 2023 (1989).
- [21] J. Guo and P.R. Berman, *Phys. Rev. A* **47**, 4128 (1993).
- [22] I. I. Sobelman, *Atomic Spectra and Radiative Transitions* (Springer-Verlag, Berlin, 1979), p. 193.
- [23] P. Domokos and H. Ritsch, *Phys. Rev. Lett.* **89**, 253003 (2002).